Solitary-wave decay and symmetry-breaking instabilities in two-mode fibers

E. M. Wright and G. I. Stegeman
Optical Sciences Center, University of Arizona, Tucson, Arizona 85721

S. Wabnitz
Fondazione Ugo Bordoni, Via Baldassarre Castiglione 59, 00144 Rome, Italy
(Received 19 June 1989)

We present a linear stability analysis for coupled nonlinear solitonlike pulses propagating in optical guiding structures supporting two linearly and/or nonlinearly coupled modes. The analytical predictions are well confirmed by numerical experiments.

I. INTRODUCTION

Optical soliton propagation in fiber waveguides supporting two distinct modes has been theoretically investigated by several authors in the past few years.[1-14] The relevance of this research effort for applications is twofold: In the context of fiber optics, optical pulses propagating as solitons were initially proposed for the transmission of information over long distances.[15] From the point of view of designing such soliton-based optical communication systems, it is of interest to evaluate what is the effect of changes in the polarization state, which unavoidably occur in standard non-polarization-preserving telecommunications fibers.[7]

On the other hand, it has recently been realized that the fast-responding nonlinearity of fibers could also provide a means of processing optical signals before detection, thus eliminating the concern that electronic bottlenecks will limit the maximum information transmission speed.[16-22] Broadly speaking, fiber-based all-optical switching elements are two-mode devices, e.g., nonlinear interferometers[16,20,22] or nonlinear couplers.[17-19,21] It has been proposed[6,23] and recently demonstrated[24] that, if the pulsed signal is coded in the form of solitons, significant improvements in the efficiency (for a given switching power) of these all-optical switches may result.

In single-mode fibers, solitons are well described by solutions of the nonlinear Schrödinger equation[15,25] (NLSE). Robustness and stability against perturbations are the characteristic of these solutions. Conversely, earlier numerical[4,13] and analytical[12] work has revealed that instabilities may occur in the propagation of solitonlike pulses in waveguides supporting two linearly coupled modes. In fact, systems of coupled NLSE's are, in general, not completely integrable by means of the inverse scattering transform,[26] so that localized solitary wave solutions do not necessarily correspond to stable bound states of an associated scattering potential. In view of the optical communication systems applications, these instabilities would clearly be detrimental. On the other hand, one might think of usefully exploiting such instabilities in soliton lasers or in soliton-based switches. For example, high-gain switches could be obtained by seeding the instability of a strong beam with a weak probe.

In earlier studies, special choices of the input conditions and of the form of the coupler were selected.[4,12,13] To be more specific, a variety of soliton instabilities (instabilities that occur using solitonlike input pulses) have been pointed out for the case of two linearly coupled NLSE's both with (birefringent fiber[4,13]) and without (nonlinear directional coupler[12]) cross-phase modulation. However, a global portrait of the different types of instability is still missing in the literature at this time. We shall present here both analytical and numerical investigations of the stability of solitary wave solutions of two coupled NLSE's which may represent a general class of two-mode fiber-optic waveguides. Our treatment will elucidate connections between earlier partial results, and, through a global analysis of the instabilities, will reveal that the picture is somewhat more complex than was pre-

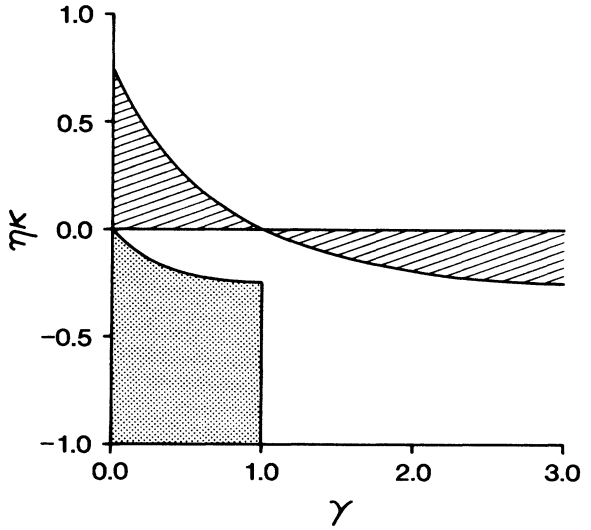

FIG. 1. Stability diagram for the solitary-wave solutions in the parameter space $(\gamma, \eta\kappa)$. The hatched (dotted) region shows the domain of instability for the solution Eq. (11) (asymmetric instability), and the dotted region shows the domain of instability for the solution of Eq. (14) (asymmetric instability).

viously appreciated. In particular, we shall identify two types of instabilities leading to either the decay of solitary waves into nonstationary solutions or to symmetry breaking.

II. COUPLED NLSE'S

We consider the situation in which, even in the presence of the nonlinearity, the field propagating in the fiber can be adequately described in terms of two linear modes of the waveguide. We therefore write the transverse electric field $\mathcal{E}(X,Y,Z,T)$ as the superposition

$$\mathcal{E}(X,Y,Z,T)=[\mathcal{E}_1(X,Y)e_1(Z,T) + \mathcal{E}_2(X,Y)e_2(Z,T)]e^{-i\omega_0 T},$$

where ω_0 is the average frequency of the pulses, and $\mathcal{E}_1 \cong \mathcal{E}_2$ are the transverse profiles of the linear guided modes of the unperturbed structure, i.e., where $e_{1,2}$ would not depend on (Z,T). In other words, we are dealing with a perturbation analysis with respect to the nearly degenerate modes $(\mathcal{E}_1,\mathcal{E}_2)$ by introducing an explicit space and time dependence in the expansion coefficients. Two distinct perturbation mechanisms contribute in determining the evolution of the field envelopes $e_{1,2}$. Firstly, a linear coupling originates either from anisotropies of the linear dielectric tensor, or from the close proximity of two parallel guiding channels. Specific examples of interest include the coupling between circular polarization modes in a birefringent fiber,[4,13,18] between linear polarizations in a periodically twisted fiber,[21] and finally, between individual waveguide modes in a directional coupler.[5,6,12,17,19] In addition, coupling and phase shifting between the modes may occur due to presence of a third-order nonlinear polarizability. Since we want to maintain the treatment here on a general level, we shall

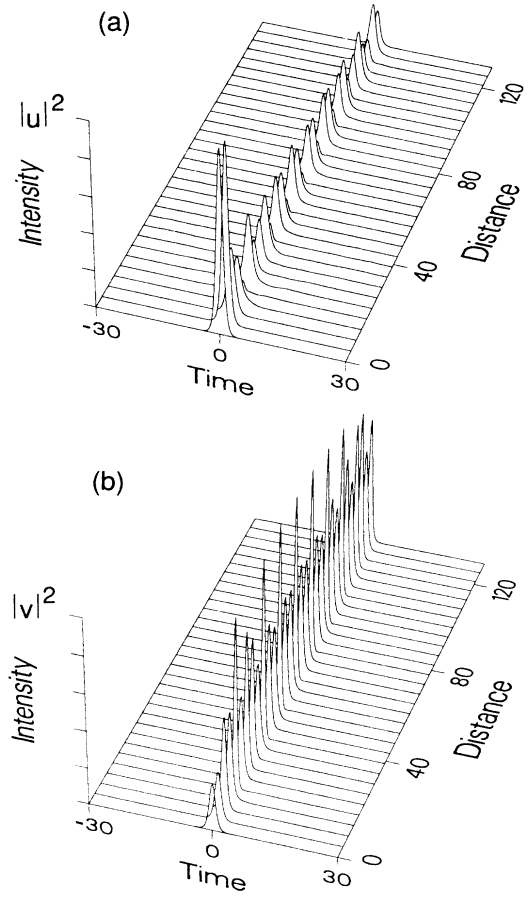

FIG. 2. (a) $|u(z,t)|^2$ and (b) $|v(z,t)|^2$, as a function of time t (with respect to a characteristic moving at the common group velocity) and scaled propagation distance z for $A_u=1$, $A_v=1.01$, $\Delta=0$, and $\eta\kappa=0.5$. The initial perturbation is asymmetric. As in all such figures, the intensity scales in (a) and (b) are in arbitrary units and are different for the two components, being normalized with respect to the peak intensity in each component.

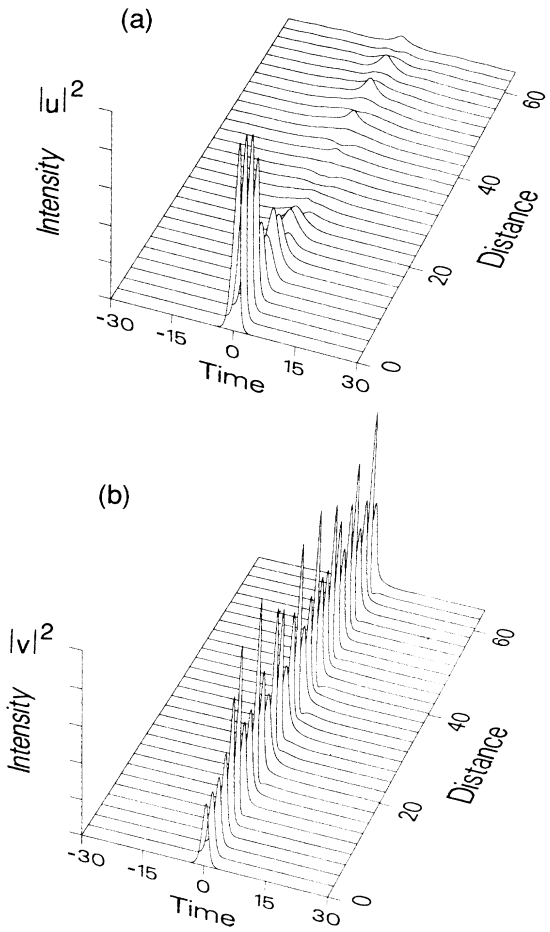

FIG. 3. As in Fig. 2, for $\eta\kappa=0.1$.

omit a derivation of the coupled-mode equations which govern the evolution of e_1 and e_2, and refer rather to the wide literature on the subject discussed above. For the most general case we shall consider the field envelopes are taken to obey the following coupled-wave equations:

$$i\frac{\partial e_1}{\partial Z}+i\frac{1}{V}\frac{\partial e_1}{\partial T}-\frac{\alpha}{2}\frac{\partial^2 e_1}{\partial T^2}+ke_2 +(R_1|e_1|^2+R_2|e_2|^2)e_1=0\ , \quad (1a)$$

$$i\frac{\partial e_2}{\partial Z}+i\frac{1}{V}\frac{\partial e_2}{\partial T}-\frac{\alpha}{2}\frac{\partial^2 e_2}{\partial T^2}+ke_1 +(R_1|e_2|^2+R_1|e_1|^2)e_2=0\ . \quad (1b)$$

where $V=(\partial\beta/\partial\omega)|_{\omega_0}^{-1}$ is the common group velocity of the copropagating modes, $\beta(\omega)$ being the frequency-dependent propagation constant, and $\alpha=(\partial^2\beta/\partial\omega^2)|_{\omega_0}^{-1}$ being the group velocity dispersion. Furthermore, $R_{1,2}$ are nonlinear coefficients which have the form $R_{1,2}=c_{1,2}\omega_0 n_2/cA_{\text{eff}}$, where n_2 is the nonlinear index coefficient, A_{eff} is the (common) effective area of the modes, and $c_{1,2}$ are numerical factors which depend on the specific form of the tensorial third-order susceptibility in each physical situation. It is convenient to rewrite Eqs. (1) in dimensionless form as

$$i\frac{\partial u}{\partial z}+\frac{1}{2}\frac{\partial^2 u}{\partial t^2}+\kappa v+(|u|^2+\gamma|v|^2)u=0\ , \quad (2a)$$

$$i\frac{\partial v}{\partial z}+\frac{1}{2}\frac{\partial^2 v}{\partial t^2}+\kappa u+(|v|^2+\gamma|u|^2)v=0\ , \quad (2b)$$

where we have specifically chosen the case of anomalous group velocity dispersion (i.e., $\alpha<0$), and we introduced the following scaled variables (soliton units):

$$t\equiv(T-Z/V)/T_s,\quad z\equiv Z/Z_c=|\alpha|Z/T_s^2\ ,$$

$$u\equiv(R_1T_s^2/|\alpha|)^{1/2}e_1,\quad v\equiv(R_1T_s^2/|\alpha|)^{1/2}e_2\ .$$

Here T_s is the pulse width of the soliton solution of the

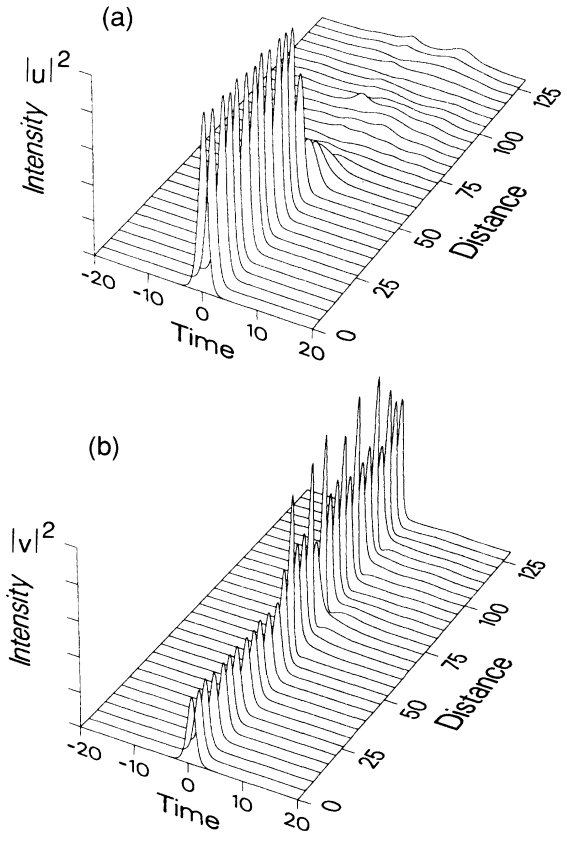

FIG. 4. As in Fig. 3, with a symmetric initial perturbation to the even solitary wave; $A_u=A_v=1$, $\Delta=0.5$.

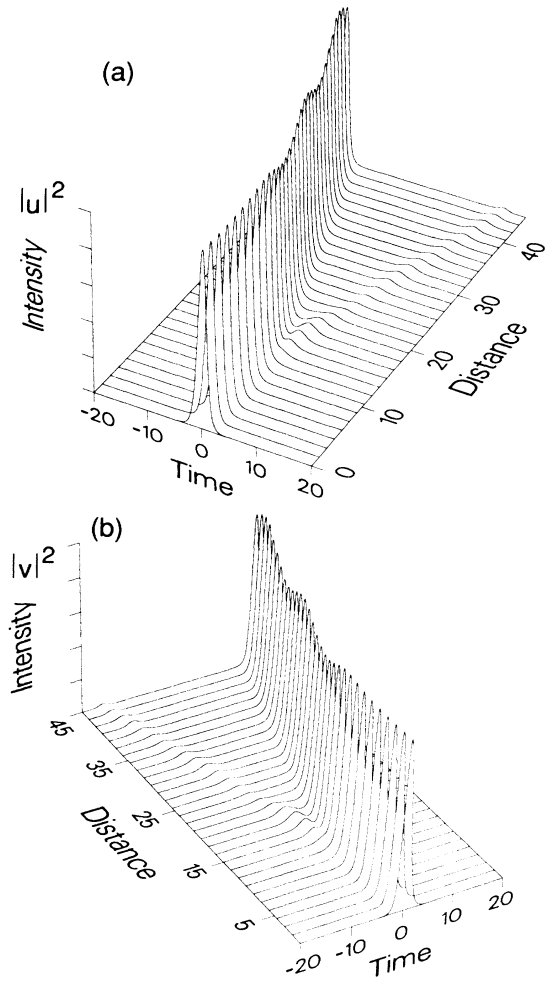

FIG. 5. Evolution of the odd solitary wave with $A_u=A_v=1$, $\eta\kappa=-0.1$, and $\Delta=0.01$.

NLSE (Ref. 1) $\kappa = kT_s^2/|\alpha|$, and $\gamma = c_2/c_1$ is the ratio between the self-phase modulation (SPM) and cross-phase modulation (CPM) contributions.

III. STABILITY ANALYSIS

In this section we shall discuss the stability of the solitary wave solutions to Eqs. (2), which can be written in the form

$$u(z,t) = e^{i\lambda z} g(t) , \tag{3a}$$

$$v(z,t) = \eta e^{i\lambda z} g(t) , \tag{3b}$$

where $\eta = \pm 1$, and $g(t)$ is taken as real without loss of generality. Since the solitary wave solutions given by Eqs. (3) correspond, in the continuous-wave limit, to the even and odd modes of the generalized nonlinear coupler described by Eqs. (2), we shall label the two solutions (3) as *even* ($\eta = +1$) and *odd* ($\eta = -1$) solitary waves. By substituting Eqs. (3) in (2) we find that the function $g(t)$ obeys

$$(\lambda - \eta\kappa)g + \frac{1}{2}\frac{\partial^2 g}{\partial t^2} + (1+\gamma)g^3 = 0 , \tag{4}$$

the solution of which can be written as

$$\lambda = \tfrac{1}{2} + \eta\kappa , \tag{5}$$

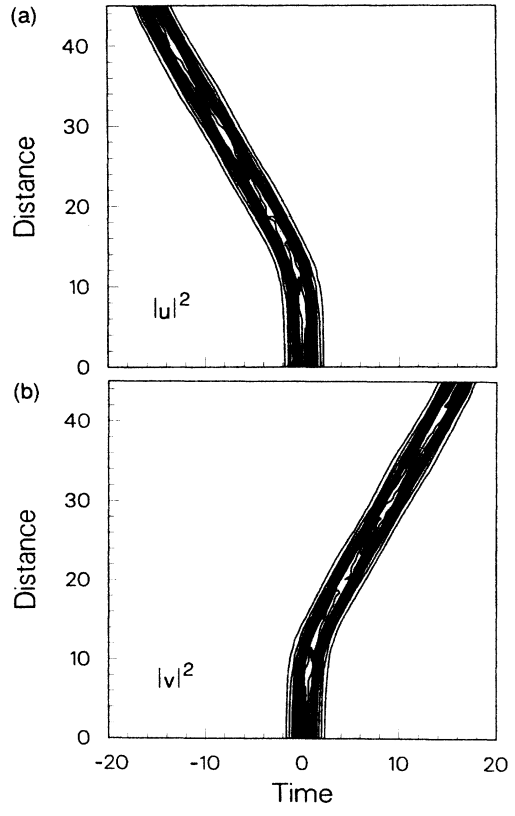

FIG. 6. Contour plot of the intensity components (a) $|u(z,t)|^2$ and (b) $|v(z,t)|^2$ for the same conditions as in Fig. 5.

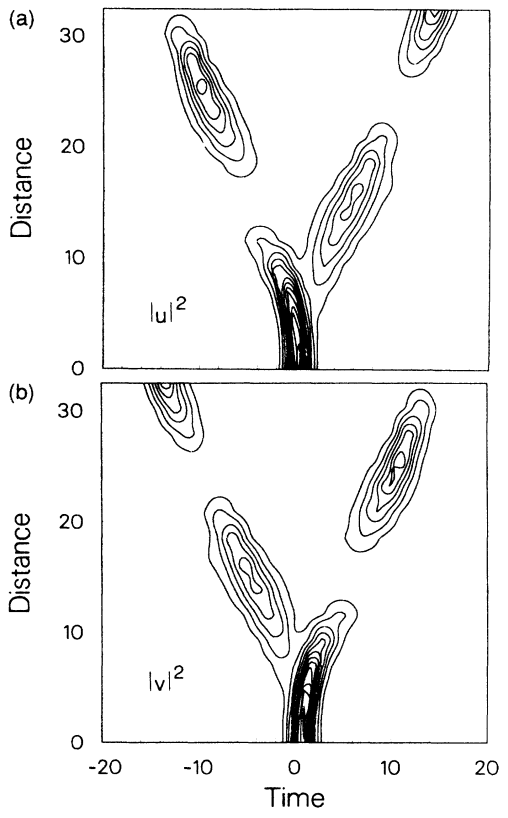

FIG. 7. As Fig. 6, with $\eta\kappa = -0.2$ and $\Delta = 0.5$.

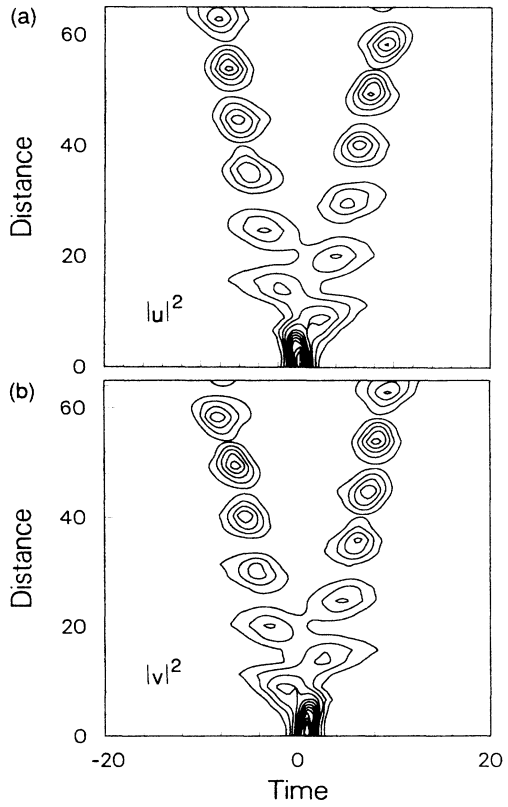

FIG. 8. As Fig. 7, with $\eta\kappa = -0.3$.

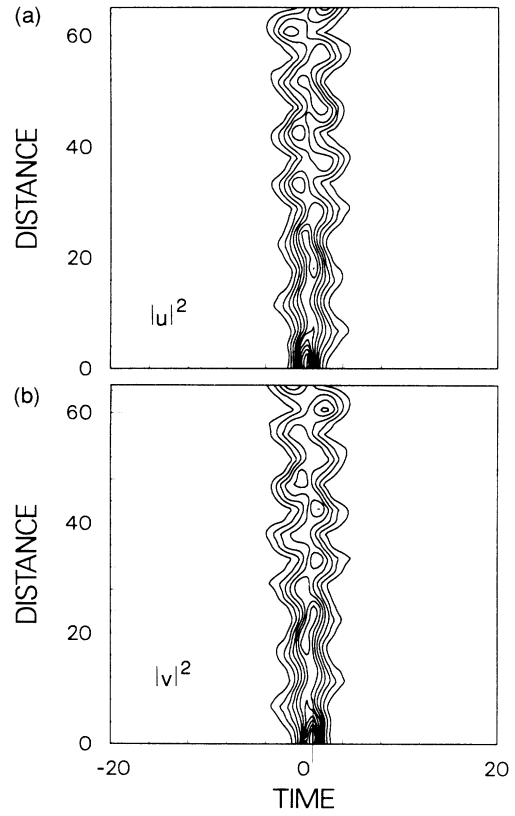

FIG. 9. As Fig. 7, with $\eta\kappa = -0.4$.

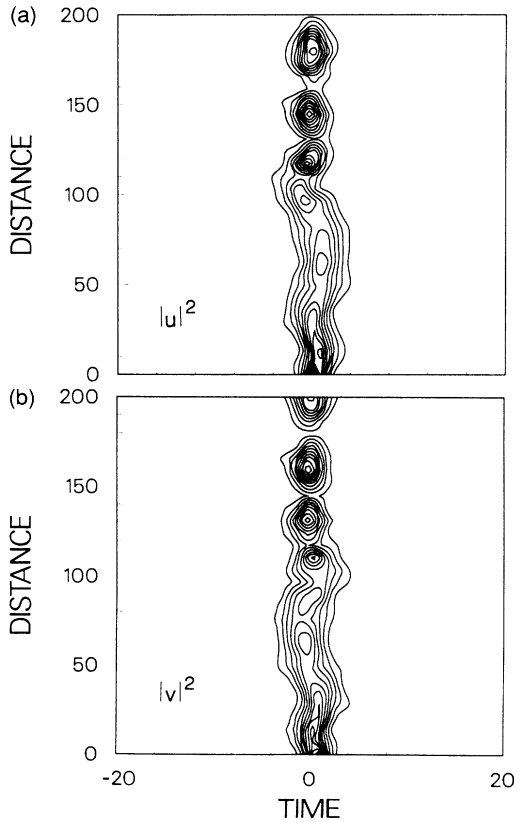

FIG. 10. As Fig. 7, with $\eta\kappa = -0.5$.

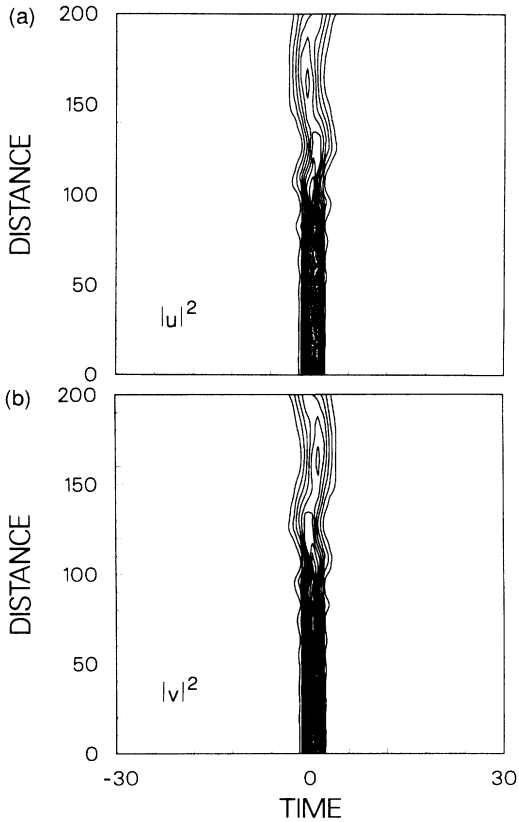

FIG. 11. As Fig. 10, with $\Delta = 0.01$.

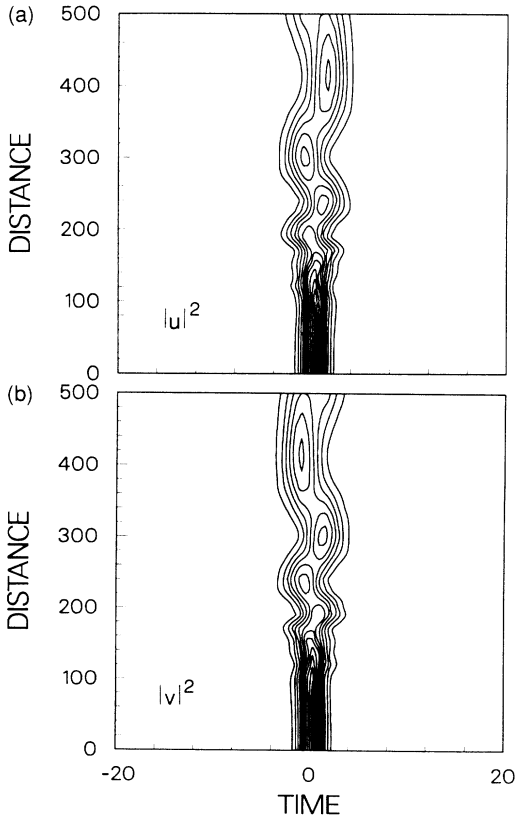

FIG. 12. As Fig. 11, with $\eta\kappa = -0.6$ and $\Delta = 0.01$.

$$g(t)=\left[\frac{1}{1+\gamma}\right]^{1/2}\mathrm{sech}(t)\ . \tag{6}$$

We consider perturbations of the solitary wave solutions of the form

$$u(z,t)=[g(t)+\epsilon(z,t)]e^{i\lambda z}\ , \tag{7a}$$

$$v(z,t)=\eta[g(t)+\Gamma(z,t)]e^{i\lambda z}\ , \tag{7b}$$

where we assume $|\epsilon|\ll 1$ and $|\Gamma|\ll 1$. By substituting Eqs. (7) in (2) and using Eqs. (2)–(7) we obtain the following linearized equations for the perturbations:

$$i\frac{\partial\epsilon}{\partial z}=\lambda\epsilon-\eta\kappa\Gamma-\frac{1}{2}\frac{\partial^2\epsilon}{\partial t^2}-g^2(\epsilon+\epsilon^*)$$
$$-\gamma g^2(\Gamma+\Gamma^*)-(1+\gamma)g^2\epsilon\ , \tag{8a}$$

$$i\frac{\partial\Gamma}{\partial z}=\lambda\Gamma-\eta\kappa\epsilon-\frac{1}{2}\frac{\partial^2\Gamma}{\partial t^2}-g^2(\Gamma+\Gamma^*)$$
$$-\gamma g^2(\epsilon+\epsilon^*)-(1+\gamma)g^2\Gamma\ . \tag{8b}$$

To proceed, we assume that both ϵ and Γ vary as $\exp(i\mu z)$ where μ is the eigenvalue. It can be shown that for eigensolutions of Eqs. (8) the eigenvalues μ are either pure imaginary or pure real. The resulting eigenvalue problem is, in general, very complicated, but some special solutions can easily be found as we shall show below. In particular, here we shall consider the stability edges for which $\mu=0$, and we set $\partial\epsilon/\partial z=\partial\Gamma/\partial z=0$ in Eqs. (8). The problem is now to find nontrivial solutions for $\epsilon(t)$ and $\Gamma(t)$ under these conditions. If we can find such solutions for a given set of parameters (e.g., γ, η, κ, etc.), this indicates that the underlying nonlinear wave may be unstable.

First we consider solutions of Eqs. (8) for which $\epsilon(t)=\Gamma(t)$, and write $\epsilon=\epsilon_R+i\epsilon_I$, to obtain

$$\frac{1}{2}\epsilon_R-\frac{1}{2}\frac{\partial^2\epsilon_R}{\partial t^2}-3(1+\gamma)g^2(t)\epsilon_R=0\ , \tag{9a}$$

$$\frac{1}{2}\epsilon_I-\frac{1}{2}\frac{\partial^2\epsilon_I}{\partial t^2}-(1+\gamma)g^2(t)\epsilon_I=0\ . \tag{9b}$$

From Eqs. (4) and (5) we see that solutions to Eqs. (9) are $\epsilon_R\propto\partial g/\partial t$, $\epsilon_I\propto g(t)$, for any combination of parameters. This solution corresponds to a neutrally stable solution which is always present.[27]

Next we consider solutions such that $\epsilon(t)=-\Gamma(t)$, which leads to the following equations:

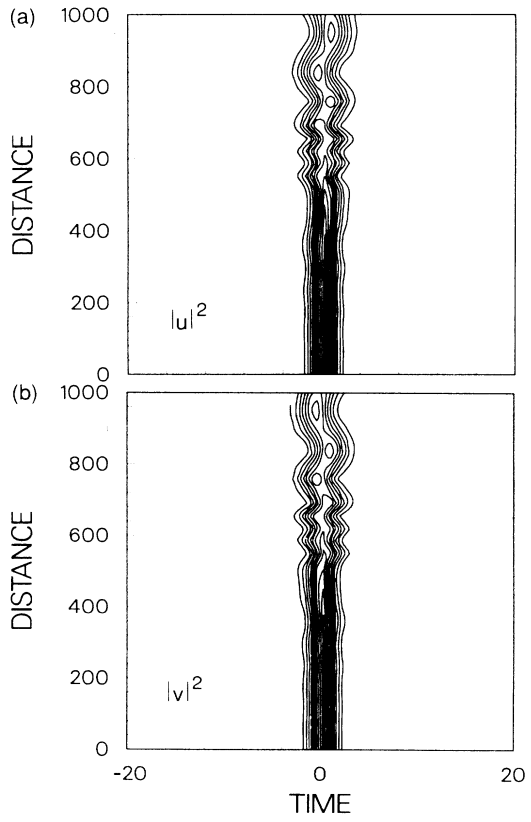

FIG. 13. As in Fig. 11, with $\eta\kappa=-1$.

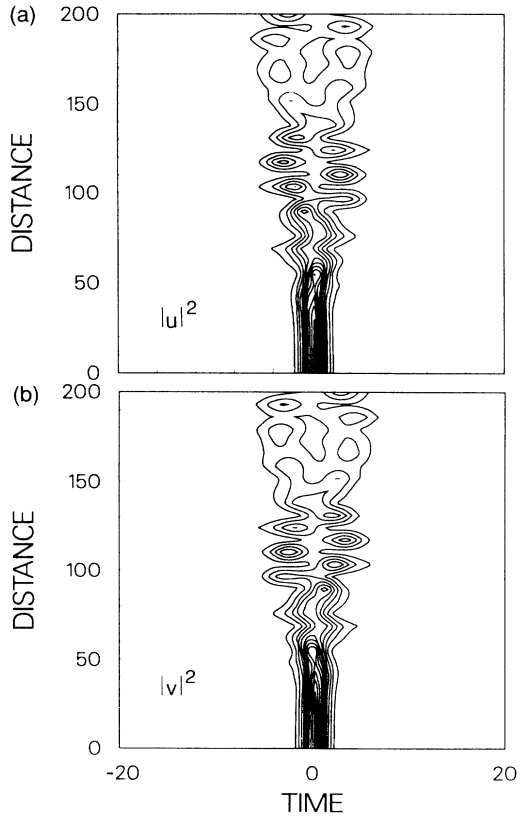

FIG. 14. Contour plot of the intensity components (a) $|u|^2$ and (b) $|v|^2$, for $\eta\kappa=-0.25$, $\gamma=0.25$, $\Delta=0.01$, and $A_u=A_v=(1+\gamma)^{-1/2}$.

$$\frac{1}{2}\epsilon_R+2\eta\kappa\epsilon_R-\frac{1}{2}\frac{\partial^2\epsilon_R}{\partial t^2}-(3-\gamma)g^2(t)\epsilon_R=0\ , \quad (10a)$$

$$\frac{1}{2}\epsilon_I+2\eta\kappa\epsilon_I-\frac{1}{2}\frac{\partial^2\epsilon_I}{\partial t^2}-(1+\gamma)g^2(t)\epsilon_I=0\ . \quad (10b)$$

For $\kappa=0$, and except for the case $\gamma=0$, a simple solution of Eqs. (10) is $\epsilon_R=0$, $\epsilon_I\propto g(t)$, which indicates that $\eta\kappa=0$ is a stability edge. [It follows from Eqs. (10) that the stability properties depend on the parameter $\eta\kappa$, which can be positive or negative.] For $\kappa\neq 0$, Eq. (10b) has the solution $\epsilon_I=0$, and (10a) has a solution of the form

$$\epsilon_R(t)=\frac{1}{\cosh^s(t)}\ . \quad (11)$$

The parameter s can be determined by substituting Eqs. (6) and (11) in (10a), which yields

$$s^2+s-\frac{6-2\gamma}{1+\gamma}=0\ , \quad (12a)$$

$$\frac{1}{2}+2\eta\kappa+\frac{s}{2}-\frac{3-\gamma}{1+\gamma}=0\ , \quad (12b)$$

from which we obtain

$$s=\frac{-1+\sqrt{1+8(3-\gamma)/(1+\gamma)}}{2}\ , \quad (13a)$$

$$\eta\kappa=\frac{1}{2}\left[\frac{3-\gamma}{1+\gamma}-\frac{1}{2}(1+s)\right]\ . \quad (13b)$$

In Eq. (13a) we have chosen the positive root since we require $s>0$ for a bounded solution [see Eq. (11)]. Equation (13a) determines the consistent value of s as a function of γ and clearly we require $\gamma<3$. Having determined s from γ using Eq. (13a), the stability edges for this solution can be determined using (13b). The stability edges for this solution are plotted in Fig. 1 in the parameter space $(\gamma,\eta\kappa)$, and includes the line $\eta\kappa=0$ as a boundary. The hatched region was found to be unstable from numerical simulations as discussed in Sec. IV.

In addition to the above solution there is also another of the form

$$\epsilon_R(t)=\frac{\sinh(t)}{\cosh^s(t)}\ , \quad (14)$$

where s is again given by Eq. (13a). In this case the stability edges are determined from

$$\eta\kappa=\frac{1}{2}\left[\frac{3-\gamma}{1+\gamma}-\frac{3s}{2}\right]\ . \quad (15)$$

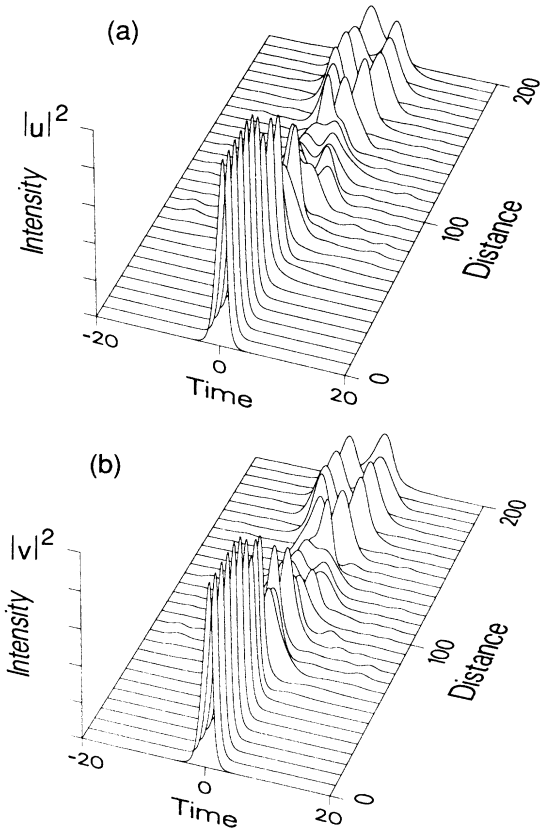

FIG. 15. Modal intensities (a) $|u|^2$ and (b) $|v|^2$, for the same conditions as in Fig. 14.

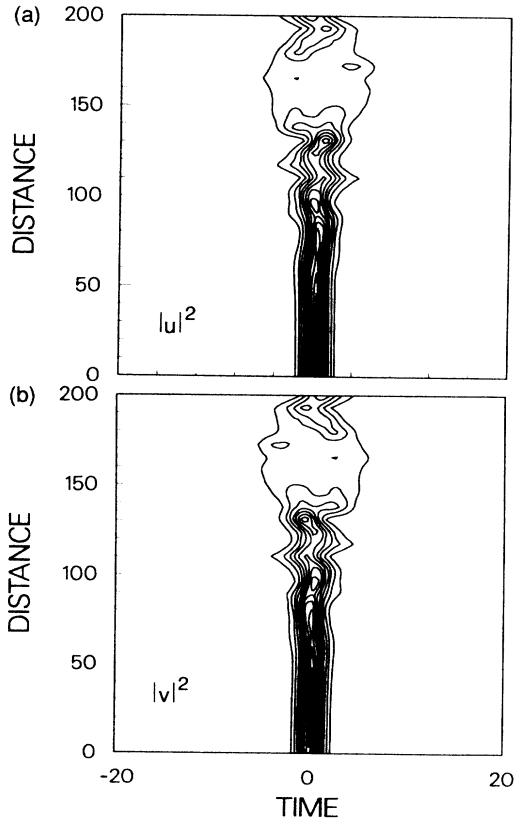

FIG. 16. As in Fig. 14, with $\gamma=0.35$.

For this solution [Eq. (14)] to be normalizable we require $s > 1$, which using Eq. (13a) becomes $\gamma < 1$. The stability edge for this solution is shown in Fig. 1, the dotted region and below being unstable. As γ approaches 1 the growth rate of the instability vanishes leading to stability with respect to this type of perturbation.

To understand the nature of the predicted instabilities we first recall that we set $\epsilon(t) = -\Gamma(t)$, so that the perturbed waves are like $u(z,t) \propto g(t) + \epsilon(t)$, $v(z,t) \propto g(t) - \epsilon(t)$. Therefore, for $\epsilon(t)$ given by Eq. (11), u and v become different as the instability grows, leading to the exchange of energy between the modes. This is a classic case of symmetry breaking since the direction in which the exchange occurs is unpredictable, and is determined by either initial seeding or fluctuations. We term this instability asymmetric since energy is exchanged between the two modes. In contrast, for $\epsilon(t)$ given by Eq. (14), the perturbed waves u and v as given above are mirror images of each other around $t = 0$. Since $g(t)$ is symmetric with respect to t, the two combinations $g(t) \pm \epsilon(t)$ correspond to two pulses whose centers are displaced symmetrically around $t = 0$: On the basis of this argument we expect that the solitary waves will break apart temporally as the instability develops. This we call the symmetric instability since no energy exchange occurs. Again this is a type of symmetry breaking, but as we shall see in Sec. IV both types of instability can also lead to nonstationary solutions.

Finally, we remark that there probably exist other types of instability for the solitary waves of Eqs. (2). Here we have found the simplest solutions and these have been verified and investigated numerically. Indeed, higher-order solutions (more field nodes) of the type discussed here are possible, but these require $\gamma < 0$, which we do not consider here. At the end of Sec. IV we present results that suggest further instabilities that are beyond the scope of the present analysis, in particular, for $\gamma = 3$.

IV. NUMERICAL RESULTS

In this section we describe numerical experiments that both support the predictions of the stability analysis summarized in Fig. 1, and reveal the nature of the instabilities. We have numerically integrated Eqs. (2) with initial conditions close to the even or odd solitary waves given

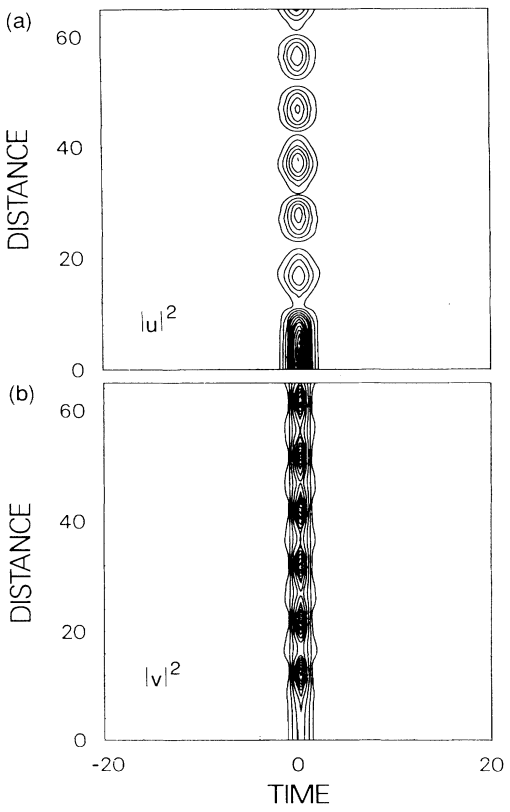

FIG. 17. Contour plot of intensities (a) $|u|^2$ and (b) $|v|^2$, for an antisymmetric perturbation to the even solitary-wave with cross-phase modulation; $\kappa = 0.2$, $\gamma = 0.2$, $\Delta = 0$, $A_u = (1+\gamma)^{-1.2} = A_v/1.01$, and $\eta = 1$.

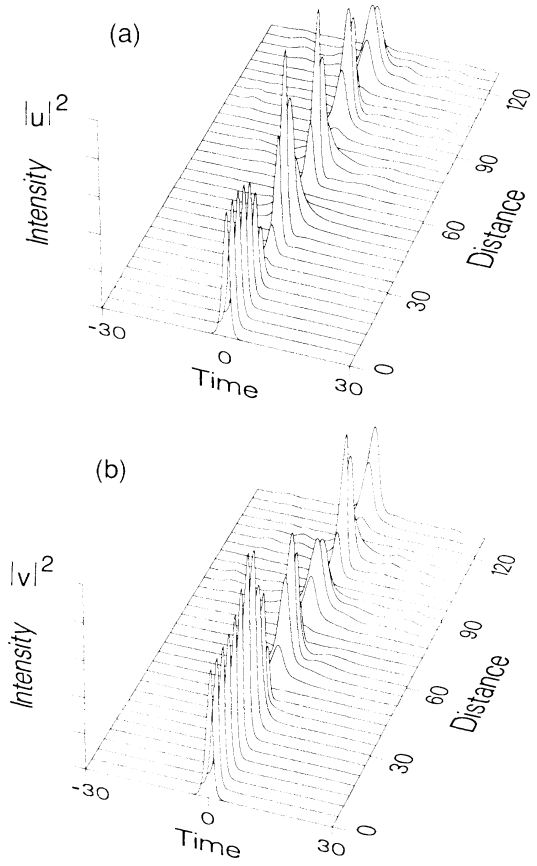

FIG. 18. Evolution of solitary-wave component intensities (a) $|u|^2$ and (b) $|v|^2$, for an antisymmetric perturbation to the odd mode. Here $\kappa = 0.125$, $\gamma = 2$, $\Delta = 0$, $A_u = (1+\gamma)^{-1/2} = A_v/1.01$, and $\eta = -1$.

by Eqs. (3). A modified version of the standard beam propagation method (BPM) was employed that was adapted to include the presence of the linear coupling. In all of the following simulations, the initial data were of the form

$$u(0,t)=A_u\,\mathrm{sech}(t-\Delta),$$
$$v(0,t)=\eta A_v\,\mathrm{sech}(t+\Delta)\ , \tag{16}$$

where $\eta=\pm 1$ as before, and $A_{u,v}>0$ are the initial amplitudes of the two waves. For the exact solitary wave solutions we have $\Delta=0$, and $A_{u,v}=A_s=\sqrt{1/(1+\gamma)}$. To produce a perturbation to the solitary waves (3), we set either $\Delta\neq 0$ and $A_{u,v}=A_s$, or $\Delta=0$, and $A_u\neq A_v$. In the first case, the initial perturbation is clearly *symmetric* in the manner discussed above, whereas the second case corresponds to an *asymmetric* perturbation of the solitary waves.

A. Linear coupling and SPM

Consider first Eqs. (2) without cross-phase modulation, i.e., set $\gamma=0$, which corresponds to the nonlinear directional coupler (NLDC). Figure 2 shows the evolution of the intensity profiles of both pulse u [Fig. 2(a)] and v [Fig. 2(b)] with propagation distance z. Here a small asymmetric input perturbation is superimposed to the even solitary wave pair with $\eta\kappa=0.5$, which should be unstable according to Fig. 1. Figure 2 shows that, following a relatively short distance, an abrupt exchange of power between the two waves occurs, which results from the exponential amplification of the initial small asymmetry. However, after a brief transient the evolution settles down into a limit cycle or quasiperiodic power-exchange regime. The amount of radiation which is emitted during the process was found to be negligible.

In contrast, Fig. 3 shows that when $\eta\kappa=0.1$, the symmetry breaking leads to almost complete and permanent energy transfer between the modes u and v. Furthermore, a relatively large amount of energy is dispersed during the collapse. Note that, in the two cases ($\eta\kappa=0.5$, 0.1), the distance over which the instability first develops remains approximately the same, in spite of the fact that for $\eta\kappa=0.1$, the edge of the stability region ($\eta\kappa=0$) is closer. We therefore observe that, when the instability is driven by an even perturbation, approaching the stability edge does not significantly affect the length, which is necessary for observing the collapse, but rather leads to qualitatively different extents in symmetry breakup.

It is also interesting to compare the evolution in Fig. 3 with that in Fig. 4, where all parameters are equal but the

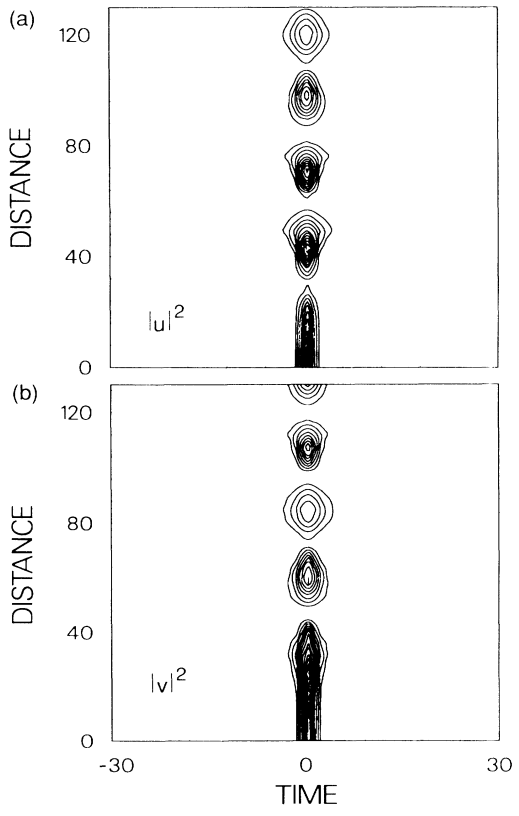

FIG. 19. Contour plot for same conditions as in Fig. 18.

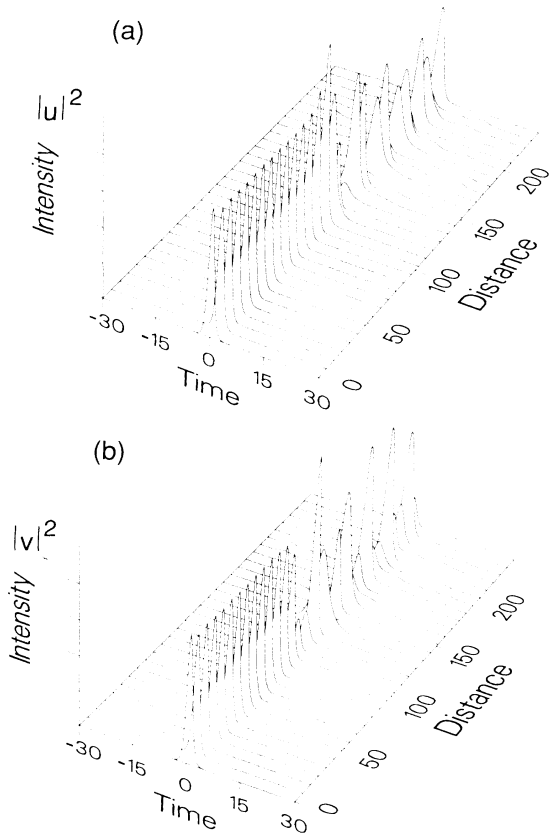

FIG. 20. As in Fig. 18, for $\eta\kappa=-0.1$, $\gamma=2$, and a symmetric perturbation to the odd solitary-wave solution with $\Delta=0.5$.

initial perturbations are asymmetric and symmetric, respectively. In each case the unstable asymmetric mode is eventually excited, but the instability takes a longer distance to develop in the second case. Clearly this is because the initial perturbation has a smaller overlap with the unstable solution. More important, however, is the observation that the evolution exhibits the same type of symmetry breaking as before, in spite of the fact that the initial perturbation is symmetric.

Figures 5–13 display the behavior of the odd-mode instability,[12] which occurs for $\eta\kappa<0$ (see Fig. 1), for different values of the coupling strength κ. As is shown in Fig. 5, given an initial slight displacement $\Delta=0.01$, for small values of $\eta\kappa$ the two solitary waves (3) repulse each other, much in agreement with the perturbative predictions of Ref. 12. However, for larger values of κ, the simple potential model[12] is inadequate for describing the behavior of the symmetric instability. By comparing Figs. 5–10, one notices the occurrence of several structural transitions in the pulse-splitting phenomenon. (In Figs. 6–13 the pulse evolution is displayed using contour plots of the pulse profiles.) Figure 5 shows that, for $|\eta\kappa|\ll 1$, a relatively small portion of the energy of each solitary wave is actually dragged along by the other pulse as they split apart, and that both pairs of waves (one strong, one weak) move at the same group velocity: One pair is advanced, the other retarded with respect to the linear group velocity. However, for $\eta\kappa<-0.145$, there is a sudden growth of this secondary component, and the initial energy of each solitary wave is split evenly between the two opposite directions (see Fig. 7). Moreover, each pair of pulses moving with the same group velocity is seen to periodically exchange energy in a manner very similar to a linear directional coupler.

Figure 8 shows that when $\eta\kappa=-0.3$, the group velocity difference between the splitting pulse pairs is reduced. Indeed, for $\eta\kappa=-0.4$ (Fig. 9), the two waves lock together and merge into a single breatherlike waveform, which is approximately time stationary (in the retarded-time reference frame). This situation is maintained when the coupling is increased even further (Fig. 10), although the waveform evolutions may become rather asymmetrical and an irregular power exchange occurs with propagation distance. Figure 11 shows the decay and the oscillatory instability which appears under the same conditions as in Fig. 10, but with a much smaller initial displacement ($\Delta=0.01$ against $\Delta=0.5$). By comparing Figs. 11–13, one observes that the solitary-wave decay route is essentially the same for larger values although the growth rate of the unstable mode is considerably reduced by increasing the strength of the linear coupling.

B. Linear coupling, SPM, and CPM

Up to this point we have examined soliton instabilities on the line $\gamma=0$, that is, in the absence of cross-phase

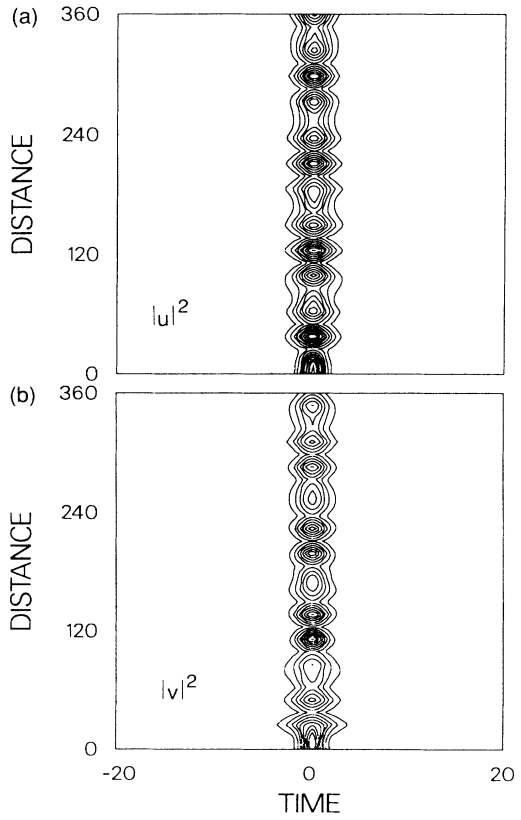

FIG. 21. Same as Fig. 18, for $\eta\kappa=-0.1$ and $\gamma=3$.

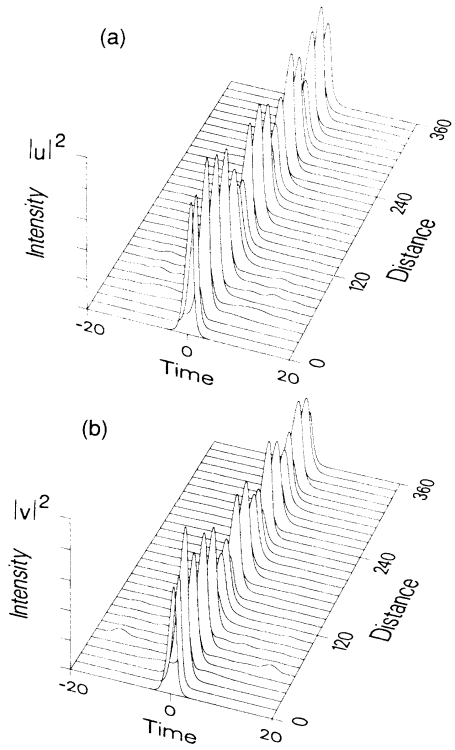

FIG. 22. Evolution of soliton component intensities (a) $|u|^2$ and (b) $|v|^2$, for the same conditions as in Fig. 21.

modulation. We shall now relax this restriction and check the predictions of the linear stability analysis for $\gamma \neq 0$ (see Fig. 1). Figures 14–17 illustrate the effect of progressively increasing the CPM (γ) with $\eta\kappa = -0.25$, which corresponds to the odd solitary wave, for the case of a symmetric perturbation ($\Delta = 0.01$). For $\gamma = 0.25$ (Figs. 14 and 15), the solitary-wave solution splits into two pairs of pulses, in a manner very reminiscent of the zero CPM case (see Fig. 8). However, at a later stage of the evolution, these localized wave packets end up decaying into a broad dispersive background. This collapse phenomena occurs at shorter propagation distances as γ is increased. This is illustrated in Fig. 16 ($\gamma = 0.35$) where the collapse is seen to occur right at the onset of instability.

Let us now consider the effect of CPM on the even-mode instabilities leading to asymmetric breakup or power exchange between the solitary-wave pairs given in Eqs. (3). When $\gamma < 1$, as occurs for example in the case of a high-birefringence rocking rotator filter[21] where $\gamma = \frac{2}{3}$, the qualitative features of the instability are similar to the $\gamma = 0$ case (compare Figs. 2 and 17). Again, Fig. 17 shows that a small initial asymmetry is amplified by the growth of the even-mode instability, leading to an exchange of energy between the waves u and v. This transient is followed by a periodic regime of interaction between the propagating pulses.

The situation appears to be rather different for $\gamma > 1$: Figs. 18–20 display symmetry breaking of the perturbed odd solitary-wave solution of Eqs. (2) with $\gamma = 2$. This corresponds to the birefringent silica fiber case, where u and v represent the circular polarization components and the unstable $\eta = -1$ solitary-wave pair represents a pulse traveling along the fast axis of the fiber.[4,8–10,13] Figures 18 and 19 show that, unlike the $\gamma = 0$ case, the instability does not lead to a permanent energy imbalance or symmetry breaking between the circular polarization modes; rather, complete power transfer between u and v modes periodically occurs along the fiber. This periodic regime, which follows the breakup, is accompanied by some energy loss into radiation.

Figure 20 shows that this type of asymptotic evolution of the instability is quite independent of the choice of a specific form for the initial perturbation. Here we have imposed a relatively strong symmetric temporal displacement $\Delta = 0.5$. The nonlinear stage of the evolution of the instability is very similar to the former case (Figs. 18 and 19).

Using numerical calculations we checked the stability edges shown in Fig. 1 and found excellent agreement with the analytical predictions. However, in our numerical study we found evidence of instabilities which are not included in our linear stability analysis. In particular, we found instabilities for $\gamma = 3$, which coincides with the results previously reported by Blow, Doran, and Wood.[4] The above results for the case $\gamma = 2$, which corresponds to the coupling of circular polarizations in silica birefringent fiber, should be compared with the findings in Ref. 4. In that work symmetry breaking involving permanent energy transfer from the fast to the slow linear polarization mode was reported. Figures 21 and 22 display solitary wave evolutions for $\gamma = 3$, with an initial asymmetrical perturbation superimposed on the odd unstable mode (fast axis mode). Some radiation is emitted during an initial transient which accompanies the decay of the coupled soliton, however, for larger propagation distances the power exchange between the circular polarization modes exhibit a quasiperodic behavior and apparently no permanent relaxation into a stable state is observed.

V. SUMMARY AND CONCLUSIONS

In this paper we have investigated the stability of coupled solitary waves in optical guiding structures supporting two linearly and/or nonlinearly coupled modes. The linear stability analysis was found to accurately predict the stability properties of the nonlinear problem, and also gave some insight into the nature of the types of instability. Numerical simulations of the nonlinear evolution equations revealed a range of phenomena including symmetry breaking and generation of nonstationary solutions.

The analysis given in this paper should provide a global understanding of the dynamics of solitons in coupled-mode problems as appear in nonlinear fiber optics. Our treatment encompasses the work of Menyuk[7] on the birefringent fiber, and that of Trillo *et al.*[11,13] and Abdullaev, Abrarov, and Darmanyan[12] on the nonlinear directional coupler. We anticipate that an extension of the present work shall incorporate the results of Blow, Doran, and Wood[4] for the birefringent fiber.

ACKNOWLEDGMENTS

This work was supported by the U.S. Air Force Office of Scientific Research (Grant No. 87-0344). The work of one of us (S.W.) was supported by a U.S. Army Research Office Grant No. DAAL01-88-K-0066 during his leave at the Optical Sciences Center, and by Fondazione Bordoni under an agreement with the Instituto Superiore Poste e Telecomunicazioni. CPU time from the John von Neumann Computer Center is gratefully acknowledged.

[1] A. L. Berkhoer and V. E. Zakharov, Zh. Eksp. Teor. Fiz. **58**, 903 (1970) [Sov. Phys.—JETP **31**, 486 (1970)].

[2] B. Crosignani, A. Cutolo, and P. Di Porto, J. Opt. Soc. Am. **72**, 1136 (1982); E. Caglioti, B. Crosignani, and P. Di Porto, Phys. Rev. A **38**, 4036 (1988).

[3] G. B. Altshuler, V. B. Karasev, S. A. Kozlov, T. A. Murina, and N. N. Rozanov, Opt. Spektrosk. **61**, 359 (1986) [Opt. Spectrosc. **61**, 228 (1986)].

[4] K. J. Blow, N. J. Doran, and D. Wood, Opt. Lett. **12**, 202 (1987).

[5] L. M. Andrushko, K. S. Karplyuk, and S. B. Ostrovsky, Radiotekh. Elektron. **32**, 427 (1987).

[6] S. Trillo, S. Wabnitz, E. M. Wright, and G. I. Stegeman, Opt. Lett. **13**, 672 (1988).

[7] C. R. Menyuk, IEEE J. Quantum Electron. **QE-23**, 174 (1987); Opt. Lett. **12**, 614 (1987); J. Opt. Soc. Am. B **5**, 392 (1988).

[8]A. D. Boardman and G. S. Cooper, J. Opt. Soc. Am. B **5**, 403 (1988).
[9]D. N. Christodoulides and R. I. Joseph, Opt. Lett. **13**, 53 (1988); D. N. Christodoulides, Phys. Lett. **132**, 451 (1988).
[10]M. V. Tratnik, and J. E. Sipe, Phys. Rev. A **38**, 2011 (1988).
[11]S. Trillo, S. Wabnitz, E. M. Wright, and G. I. Stegeman, Opt. Lett. **13**, 871 (1988).
[12]F. Kh. Abdullaev, R. M. Abrarov, and S. A. Darmanyan, Opt. Lett. **14**, 131 (1989).
[13]S. Trillo, S. Wabnitz, E. M. Wright, and G. I. Stegeman, Opt. Commun. **70**, 166 (1989).
[14]S. Trillo and S. Wabnitz, J. Opt. Soc. Am. **6**, 238 (1989).
[15]A. Hasegawa and F. Tappert, Appl. Phys. Lett. **23**, 142 (1973).
[16]R. H. Stolen and A. Ashkin, Appl. Phys. Lett. **22**, 294 (1973).
[17]D. D. Gusovskii, E. M. Dianov, A. A. Maier, V. B. Neustreuev, E. I. Shklovskii, and A. Shcherbakov, Sov. J. Quantum Electron. **15**, 1523 (1985); D. D. Gusovskii, E. M. Dianov, A. A. Maier, V. B. Neustreuev, V. V. Osiko, A. M. Prokhorov, K. Yu. Sitarkii, and A. Shcherbakov, *ibid.* **17**, 724 (1987).
[18]S. Trillo, S. Wabnitz, R. H. Stolen, G. Assanto, C. T. Seaton, and G. I. Stegeman, Appl. Phys. Lett. **49**, 1224 (1986).
[19]S. R. Friberg, Y. Silberberg, M. K. Oliver, M. J. Andrejco, M. A. Saifik, and P. W. Smith, Appl. Phys. Lett. **51**, 1135 (1987); S. R. Friberg, A. M. Weiner, Y. Silberberg, B. G. Sfez, and P. W. Smith, Opt. Lett. **13**, 904 (1988).
[20]M. N. Islam, S. P. Dijaili, and J. P. Gordon, Opt. Lett. **13**, 518 (1988).
[21]S. Trillo, S. Wabnitz, N. Finlayson, W. C. Banyai, C. T. Seaton, G. I. Stegeman, and R. H. Stolen, Appl. Phys. Lett. **53**, 837 (1988); S. Trillo, S. Wabnitz, W. C. Banyai, N. Finlayson, C. T. Seaton, G. I. Stegeman, and R. H. Stolen, IEEE J. Quantum Electron. **QE-25**, 104 (1989).
[22]M. J. LaGasse, D. Liu-Wong, J. C. Fujimoto, and H. A. Haus, Opt. Lett. **14**, 311 (1989).
[23]N. J. Doran and D. Wood, J. Opt. Soc. Am. B **4**, 1843 (1987).
[24]K. J. Blow, N. J. Doran, and B. K. Nayar, in *Technical Digest of the Topical Meeting on Nonlinear Guided-Wave Phenomena* (Optical Society of America, Washington, D.C., 1989), paper PD7; M. N. Islam, E. R. Sunderman, R. H. Stolen, W. Pleibel, and J. R. Simpson, *ibid.*, paper PD8.
[25]V. E. Zakharov and A. B. Shabat, Zh. Eksp. Teor. Fiz. **36**, 61 (1971).
[26]V. E. Zakharov and E. I. Schulman, Physica **4D**, 270 (1982); R. Sahadevan, K. M. Tamizhmani, and M. Lakshmanan, J. Phys. A **19**, 1783 (1986).
[27]V. E. Zakharov and A. M. Rubenchik, Zh. Eksp. Teor. Fiz. **65**, 997 (1973) [Sov. Phys.—JETP **38**, 494 (1974)].